

Fabricating Ferromagnetic MoS₂ Based Composite Exposed to Simulated Sunlight for Sodium Storage

Fusheng Liu,^{a,b} Yaoyao Xiao,^{a,b} Pinyu Han,^{a,b} Yuting Liu,^{a,b} Guohui Qin^{*a,b}

^a State Key Laboratory Base for Eco-Chemical Engineering, College of Chemical Engineering, Qingdao University of Science and Technology, Qingdao 266042, Shandong, China

^b Shandong Collaborative Innovation Center of Eco-Chemical Engineering, Qingdao 266042, China

Corresponding author.

E-mail: guohuiq163@sina.com

Directory of contents

Fig.S1 (a) The folded free standing active material circular disc, (b) The punched battery case, (c) The fabricated battery isolated from the air conditions, (d) The optical photograph of one fabricated battery exposed to simulated sunlight undergone LAND battery test and (e), (f) their corresponding amplified schematic pictures.

Fig. S2 (a) N₂ adsorption and desorption isotherm and (b) pore size distribution of Fe@C@CQD@MoS₂.

Fig.S3 (a) Ultraviolet-visible light absorption spectrum of pure MoS₂ and Fe@C@CQD@MoS₂, (b) The CV comparison images of Fe@C@CQD@MoS₂ and Fe@C@MoS₂.

Fig.S4 (a) and (b) high-magnification TEM image of Fe@C@CQD@MoS₂ nanoparticles after exposed to simulated sunlight 2 min and 200 cycles, (c) schematic evolution of the SEI reactivation.

Fig. S5 XPS spectrum of 2H and 1T MoS₂ at different time.

Fig. S6 Na migration pathways and barriers for Fe@C@MoS₂.

Fig. S7 The charge and discharge profiles of Fe@C@CQD@MoS₂ for repeated 100 cycles.

Fig. S8 The SEM images of (a) Fe@C@MoS₂ (b) Fe@C@CQD@MoS₂ before and after 100 cycles .

Fig. S9 The calculated SEI film variation according to comsol multiphysics model.

Fig. S10 The TEM image comparison of (a) Fe@C@CQD@MoS₂ and (b) Fe@C@MoS₂ after 500th cycles at 500 mAg⁻¹.

Fig. S11 CV profiles of capacitive contribution at scan rates from 0.1 to 2 mV/s (a-e). (f) Specific capacities generated from battery contribution and capacitive contribution at different scan rates for Fe@C@CQD@MoS₂.

Fig. S12 The PL comparison files of Fe@C@CQD@MoS₂ and C@CQD@MoS₂.

Fig. S13 The temperature variation base on such Fe@C@CQD@MoS₂, C@CQD@MoS₂ as time increases.

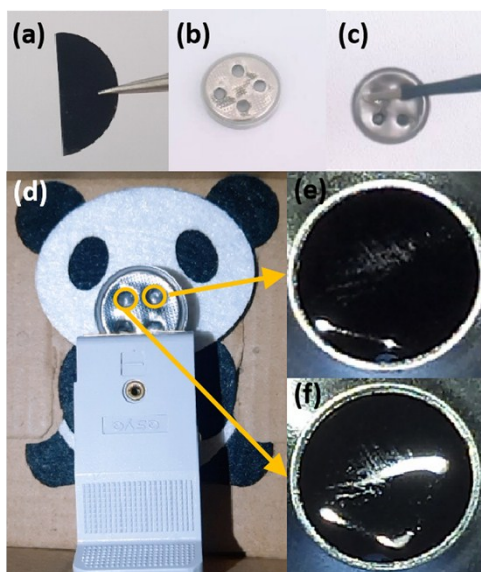


Fig. S1 (a) The folded free standing active material circular disc, (b) The punched battery case, (c) The fabricated battery isolated from the air conditions, (d) The optical photograph of one fabricated battery exposed to simulated sunlight undergone LAND battery test and (e), (f) their corresponding amplified schematic pictures.

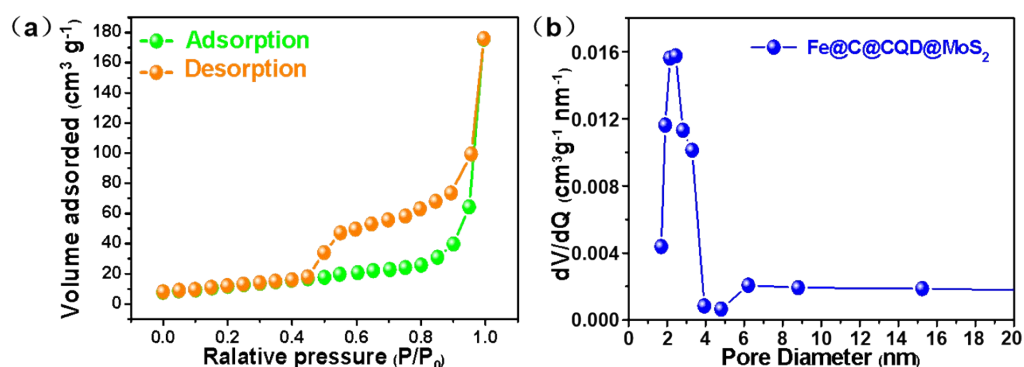


Fig. S2 (a) N_2 adsorption and desorption isotherm and (b) pore size distribution of $Fe@C@CQD@MoS_2$.

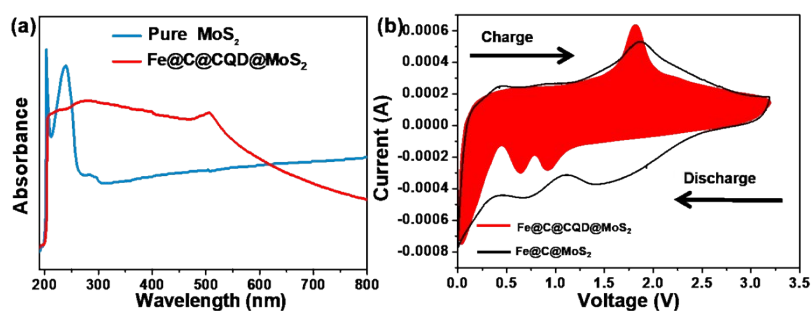


Fig.S3 (a) Ultraviolet-visible light absorption spectrum of pure MoS_2 and $Fe@C@CQD@MoS_2$, (b) The CV comparison images of $Fe@C@CQD@MoS_2$ and $Fe@C@MoS_2$.

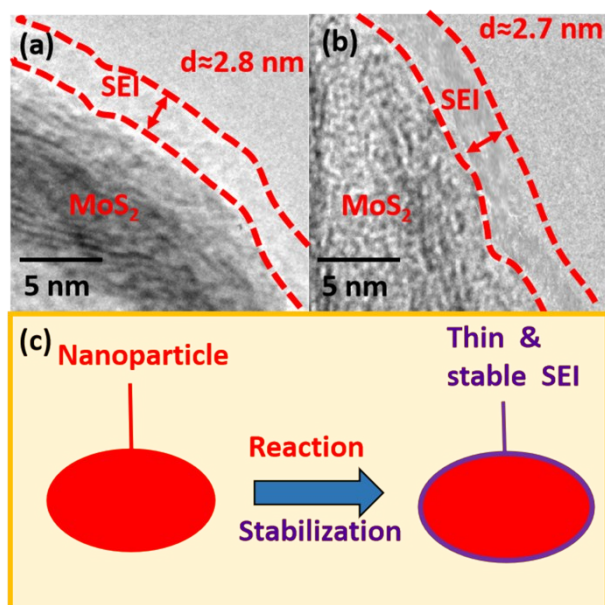


Fig.S4 (a) and (b) high-magnification TEM image of Fe@C@CQD@MoS₂ nanoparticles after exposed to simulated sunlight 2 min and 200 cycles, (c) schematic evolution of the SEI reactivation.

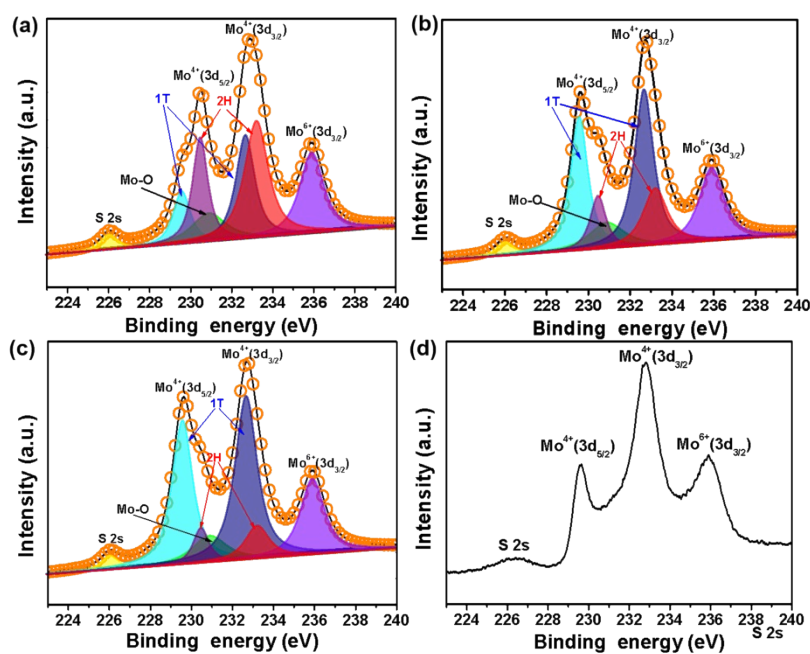


Fig. S5 XPS spectrum of 2H and 1T MoS₂ at different time.

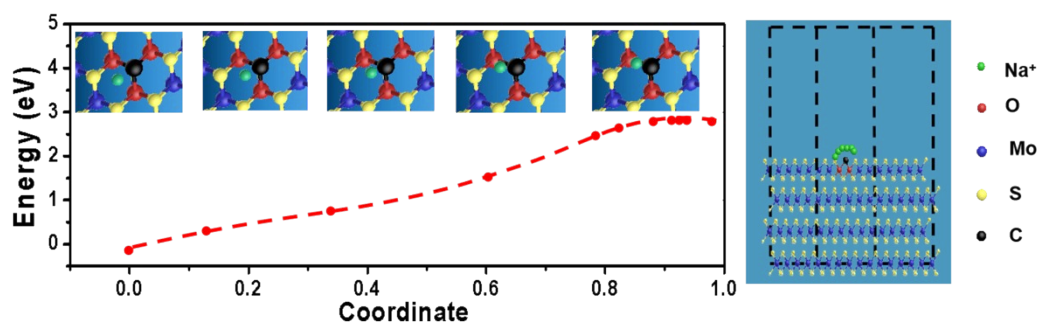


Fig. S6 Na migration pathways and barriers for Fe@C@MoS₂.

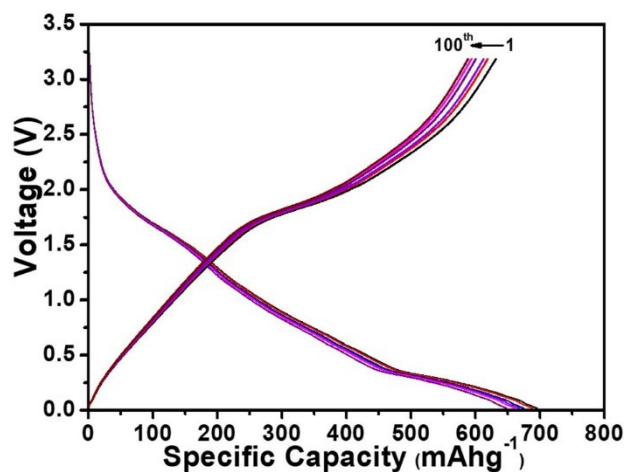


Fig. S7 The charge and discharge profiles of Fe@C@CQD@MoS₂ for repeated 100 cycles.

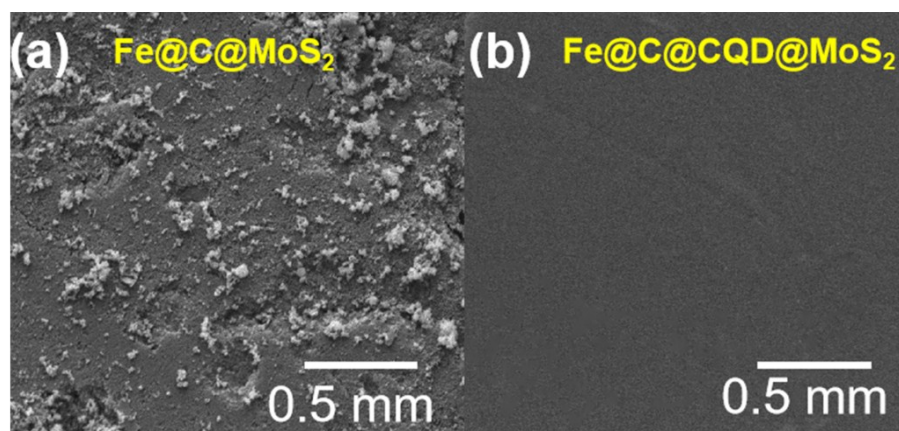


Fig. S8 The SEM images of collectors (a) Fe@C@MoS₂ (b) Fe@C@CQD@MoS₂.

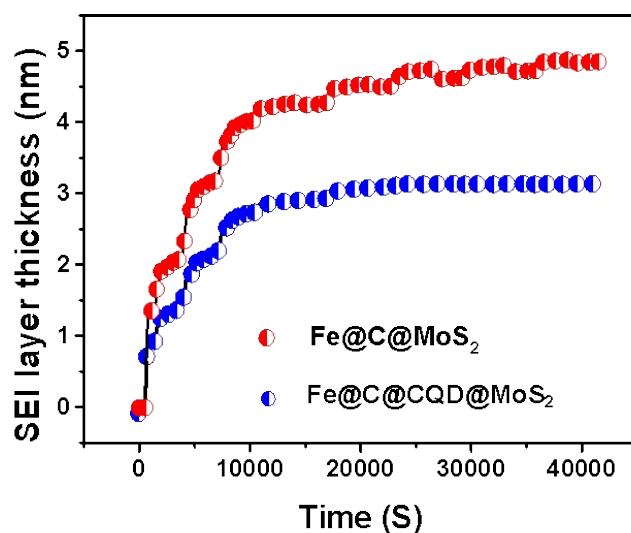


Fig. S9 The calculated SEI film variation according to comsol multiphysics model.

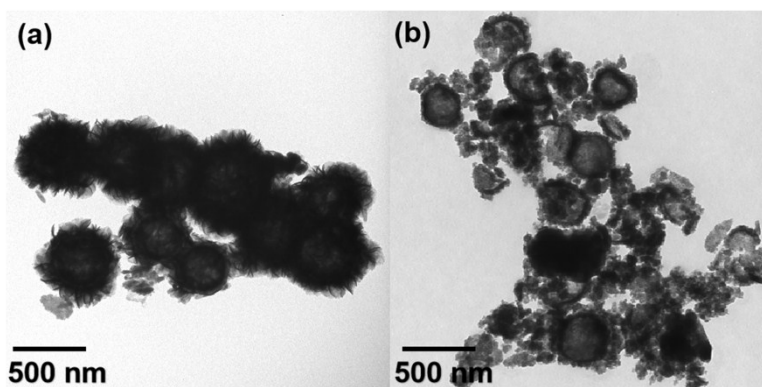


Fig. S10 The TEM image comparison of (a) Fe@C@CQD@MoS₂ and (b) Fe@C@MoS₂ after 500th cycles at 500 mAg⁻¹.

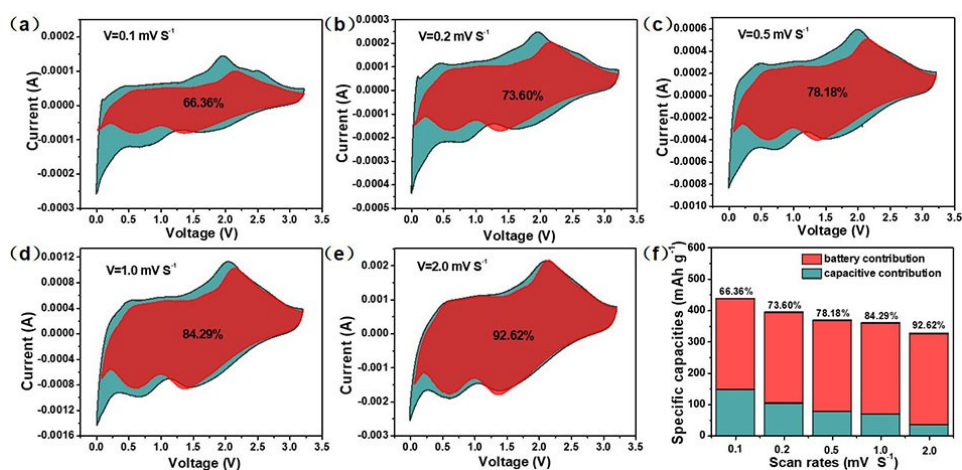


Fig. S11 CV profiles of capacitive contribution at scan rates from 0.1 to 2 mV/s (a-e). (f) Specific capacities generated from battery contribution and capacitive contribution at different scan rates for Fe@C@CQD@MoS₂.

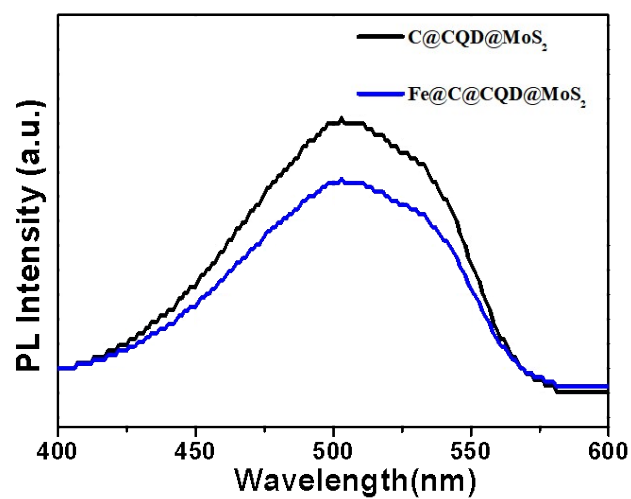


Fig. S12 The PL comparison files of Fe@C@CQD@MoS₂ and C@CQD@MoS₂.

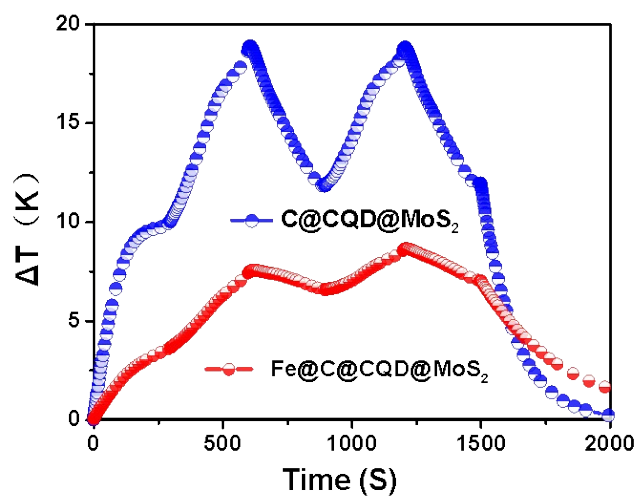


Fig. S13 The temperature variation base on such Fe@C@CQD@MoS₂, C@CQD@MoS₂ as time increases.